ApJ Letters, in press

A New 3.25 Micron Absorption Feature toward Mon R2/IRS-3

K. Sellgren

Department of Astronomy, Ohio State University, 174 West 18th Av., Columbus, OH 43210 USA
e-mail: sellgren@payne.mps.ohio-state.edu

T. Y. Brooke

Jet Propulsion Laboratory, M/S 169–237, 4800 Oak Grove Dr., Pasadena, CA 91109 USA
e-mail: tyb@scn5.jpl.nasa.gov

R. G. Smith

Department of Physics, University College, University of New South Wales, Australian Defence Force Academy, Canberra ACT 2600, Australia
e-mail: rgs@phadfa.ph.adfa.oz.au

T. R. Geballe

Joint Astronomy Centre, 660 N. Aohoku Place, University Park, Hilo, HI 96720
e-mail: tom@jach.hawaii.edu

Abstract

A new 3.2–3.5 μm spectrum of the protostar Mon R2/IRS-3 confirms our previous tentative detection of a new absorption feature near 3.25 μm. The feature in our new spectrum has a central wavelength of 3.256 μm (3071 cm^{-1}) and has a full-width at half maximum of 0.079 μm (75 cm^{-1}). We explore a possible identification with aromatic hydrocarbons at low temperatures, which absorb at a similar wavelength. If the feature is due to aromatics, the derived column density of C–H bonds is $\sim 1.8 \times 10^{18}$ cm^{-2}. If the absorbing aromatic molecules are of roughly the same size as those responsible for aromatic emission features in the interstellar medium, then we estimate that $\sim$9% of the cosmic abundance of carbon along this line of sight would be in aromatic hydrocarbons, in agreement with abundance estimates from emission features.

Subject headings: infrared: general — ISM: dust, extinction — ISM: molecules — stars: pre-main sequence

1. Introduction

The C–H stretch absorptions of many of the organic molecules expected to be formed or condensed on molecular cloud dust lie in the 3.2–3.6 μm region, on the long wavelength side of the 3.1 μm H_2O ice band which dominates the spectrum of embedded sources. Sellgren, Smith, & Brooke (1994) recently reported a tentative detection of a new absorption feature at 3.25 μm (3078 cm^{-1}) toward Mon R2/IRS-3, a protostar in the Mon R2 star formation region (Beckwith et al. 1976). Their spectrum had a resolution $\lambda/\Delta\lambda \approx 720$ at 3.25 μm. Here, we present a new spectra of Mon R2/IRS-3 with a resolution of 1000 which confirms the presence of a 3.25 μm feature. Some possible identifications are discussed.

2. Observations

The latest observations of Mon R2/IRS-3 were made on 1994 October 8 at the United Kingdom Infrared Telescope (UKIRT) on Mauna Kea. The CGS4 long-slit spectrometer (Mountain et al. 1990) was used with the 75 lines mm^{-1} grating in first order and the 300-mm focal length camera. This provided a wavelength resolution of 0.0033 μm ($\lambda/\Delta\lambda$ = 1000 at 3.25 μm). The spectrometer is designed to have only one resolution element per pixel, so improved sampling of the spectrum was obtained by moving the detector by one-third of a resolution element between individual spectra and repeating this until two resolution elements were observed by each pixel. The observations consist of two overlapping grating positions, at 3.16–3.37 μm and 3.34–3.55 μm. The pixel size was 1.55$''$. The spectrometer slit was 90$''$ $\times$ 1.55$''$ with the long direction oriented east-west. The sources were nodded $\sim$12$''$ along the slit for background subtraction. An argon spectrum in second order was used for wavelength calibration. We compared our spectrum of Mon R2/IRS-3 with the star HR 1948 (O9Iab:) for atmospheric cancellation. The airmass difference between Mon R2/IRS-3 and HR 1948 was always less than 0.03.

In the final spectra, several points at 3.313 – 3.321 μm affected by strong telluric CH_4 have been removed. We have also removed points near 3.297 μm which may have been affected by any photospheric Pfund δ feature in the O9Iab: atmospheric comparison star.

3. Results

The new spectrum of Mon R2/IRS-3 is shown in Figure 1. The observations fall in the region of the 3.1 μm H_2O ice band and the broad absorption wing which peaks near 3.3–3.4 μm (Smith, Sellgren, & Tokunaga 1989). The intrinsic spectral shape of this absorption is uncertain. Thus the best continuum to use for deriving the optical depth of narrow absorption features in this region is a local continuum which passes smoothly through those parts of the spectrum not containing narrow absorption features. We have fit a second-order polynomial to the spectrum of Mon R2/IRS-3, excluding data at 3.2–3.3 μm and longward of 3.4 μm from the fit. The choice of excluded regions is the same as that used by Sellgren et al. (1994). Our adopted continuum is shown as a solid line in Figure 1.

The derived optical depth is also shown in Figure 1. We fit two Gaussians to the optical depth curve. The central wavelength, full width at half-maximum (FWHM), and optical depth of each Gaussian were varied to produce the best fit to our observations. We derive central wavelengths of 3.256 $\pm$ 0.003 μm and 3.484 $\pm$ 0.003 μm (3071 $\pm$ 3 cm^{-1} and 2870 $\pm$ 2 cm^{-1}) for the 3.25 μm and 3.48 μm features, respectively. We also find FWHM values of 0.079 $\pm$ 0.007 μm and 0.117 $\pm$ 0.007 μm (75 $\pm$ 6 cm^{-1} and 97 $\pm$ 6 cm^{-1}) for the 3.25 μm and 3.48 μm features, respectively. Our new measurements of the central wavelengths and widths agree well with those of Sellgren et al. (1994). The 3.25 μm optical depth we measure, 0.045, also agrees well with Sellgren et al. (1994). The 3.48 μm optical depth we derive, 0.058, does not agree with the value of 0.036 measured by Sellgren et al. (1994). However, the optical depth is sensitive to the choice of continuum, so the Sellgren et al. (1994) spectrum provides the most reliable value for the 3.48 μm optical depth because the current spectrum (Fig. 1) does not extend to long enough wavelengths to provide continuum on the long wavelength side of the 3.48 μm feature.

4. Discussion

The 3.48 μm feature was first identified by Allamandola et al. (1992) toward four protostars. They attributed the feature to C–H bonds in hydrocarbons with "diamond-like" bonding. This feature in Mon R2/IRS-3 and other sources is discussed in more detail by Brooke, Sellgren, & Smith (1995).

Standard references on room temperature infrared spectra suggest that the 3.25 μm feature might be due to a C–H stretch of the $=CH_2$ group in an alkene, which occurs at

3.23–3.25 μm (e.g. Williams & Fleming 1987). An alkene identification, however, is unlikely because alkenes have a second, comparably strong, feature at 3.29–3.32 μm which is not observed toward Mon R2/IRS-3. We have searched the low temperature laboratory spectra of pure ices and ice mixtures with compositions thought to be appropriate to molecular clouds (d'Hendecourt & Allamandola 1986; Grim et al. 1989; Hudgins et al. 1993). These spectra reveal no obvious absorption features near 3.25 μm.

We suggested earlier (Sellgren et al. 1994) that the 3.25 μm feature may be due to absorption by aromatic hydrocarbons at low temperature, based on a similarity in wavelength to the C–H stretch of polycyclic aromatic hydrocarbons (PAHs) isolated in neon matrices at a temperature of 4.2 K (Joblin et al. 1994). The aromatic C–H stretch wavelength is a function of temperature, increasing with increasing temperature (Colangeli, Mennella, & Bussoletti 1992; Joblin et al. 1994, 1995). Aromatic hydrocarbons are a promising candidate for the 3.25 μm absorption feature, since aromatic emission features at 3.3, 6.2, 7.7, 8.6, and 11.3 μm have been observed throughout the interstellar medium of our own and other galaxies. Corresponding *absorption* features have been searched for, but until now have not been definitely detected in molecular clouds. The infrared emission features have been attributed to a variety of aromatic substances, including hydrogenated amorphous carbon (HAC) grains (Blanco, Bussoletti, & Colangeli 1988; Ogmen & Duley 1988), PAHs (Léger & Puget 1984; Allamandola, Tielens, & Barker 1985), quenched carbonaceous composite (QCC) grains (Sakata et al. 1987), and other aromatic materials (see Sellgren 1994 for a review of proposed identifications).

We compare in Table 1 the observed wavelength of the 3.25 μm feature toward Mon R2/IRS-3 with the wavelengths of several aromatic substances. We list in Table 1 the measured wavelengths of solid QCC (Sakata et al. 1990), the 3.3 μm interstellar aromatic emission feature (Tokunaga et al. 1991), the PAH molecule coronene in the condensed phase and the gas-phase (Flickinger, Wdowiak, & Gómez 1991), solid HAC (Biener et al. 1994), and the PAH molecules coronene and pyrene isolated in a neon matrix (Joblin et al. 1994).

Joblin et al. (1995) have examined the temperature dependence of the C–H stretch wavelength of gas-phase aromatic molecules in detail. They state that the wavelength increases with increasing temperature due to anharmonic coupling of the C–H stretch mode with excited longer wavelength modes. In Table 1 we also present the predicted wavelengths for each aromatic material, when shifted from the temperature at which the measurement was made to a temperature of 80 K, appropriate for the icy grains toward Mon R2/IRS-3 (Smith et al. 1989), using Eq. 5 of Joblin et al. (1995) and the assumption that the neon matrix does not introduce a wavelength shift from the gas phase. The temperature dependence of the aromatic C–H stretch wavelength (Joblin et al. 1995) was derived for gas-phase aromatic molecules, and we caution that solid-phase aromatics, such as HAC or QCC, may not follow the same relation.

In Figure 1, we compare the optical depth profile of the 3.25 μm absorption feature and the profile of the 3.3 μm aromatic interstellar emission feature in IRAS 21282+5050 (Nagata et al. 1988), after continuum subtraction (Tokunaga et al. 1991), and after shifting the center of the emission feature to the predicted wavelength at 80 K (see Table 1). The two feature profiles show reasonable agreement, although since the width of each feature is probably dominated by different processes, such agreement may be fortuitous.

The average of the observed feature wavelengths from this paper and Sellgren et al. (1994) is 3.253 $\pm$ 0.004 μm, which is shorter than the aromatic hydrocarbon wavelengths in Table 1 by 0.004–0.032 μm. The fact that the 3.25 μm absorption feature just barely overlaps the short wavelength side of the range of cold aromatic hydrocarbon wavelengths presents a problem, since moving the aromatic C–H vibration to shorter wavelengths (higher frequencies) means strengthening the C–H bond, something that seems difficult to achieve if the aromatic hydrocarbons are immersed in an ice matrix of some sort.

Any identification of the 3.25 μm feature at this time rests only on one absorption feature, and the wavelength match with aromatic hydrocarbons is not exact. A search for the longer wavelength features associated with aromatic hydrocarbons would provide one test of this identification.

If we assume that the 3.25 μm absorption feature is due to aromatic hydrocarbons, the column density of aromatic C–H bonds along the line of sight to Mon R2/IRS-3 can be estimated. Measurements of aromatic hydrocarbons in absorption are important because estimates of the abundance of aromatic hydrocarbons from the observed emission features (Allamandola et al. 1989; Puget & Léger 1989; Joblin, Léger, & Martin 1992) are much less straightforward.

To estimate the column density of aromatic C–H bonds, we use the relation, $N \simeq \tau\Delta\nu/A$, where τ is the maximum optical depth of the 3.25 μm absorption feature, $\Delta\nu$ is the feature FWHM in cm^{-1}, A is the integrated absorbance, and N is the derived column density of molecular bonds (Allamandola et al. 1992). An average of the results of this paper and Sellgren et al. (1994) gives $\tau(3.25\ \mu\mathrm{m}) = 0.047$ and $\Delta\nu = 66$ cm^{-1} for the 3.25 μm feature. For the three aromatic molecules, pyrene, coronene, and ovalene, studied by Joblin et al. (1994), the value of A per aromatic C–H bond for the 3.25 μm feature was 0.7–1.4 $\times$ 10^{-18} cm bond^{-1} in the solid phase and 2.1–4.1 $\times$ 10^{-18} cm bond^{-1} in the gas phase. We average over all three molecules in both phases, to estimate an average value of

$A = 1.7 \times 10^{-18}$ cm bond^{-1}. We thus derive a column density of aromatic C–H bonds of N(C–H) $\sim 1.8 \times 10^{18}$ bonds cm^{-2} along the line-of-sight.

The abundance by number of aromatic C–H bonds, X(C–H), is the ratio of the column density of aromatic C–H bonds divided by the total hydrogen column density, N_H. We estimate N_H in two ways. The silicate optical depth, $\tau(9.7\ \mu\mathrm{m}) = 4.3$, observed toward Mon R2/IRS-3 (Willner et al. 1982) implies $A_V = 80$ mag assuming $\mathrm{A}_V/\tau(9.7\ \mu\mathrm{m}) = 18.5$ (Mathis 1990). However, $\mathrm{A}_V/\tau(9.7\ \mu\mathrm{m})$ is observed to vary by a factor of two (Mathis 1990). An independent estimate of A_V comes from the 4.6 μm ^{13}CO gas absorption observed toward Mon R2/IRS-3 (Mitchell 1995), which gives $N(^{13}\mathrm{CO}) = 1.6 \times 10^{17}$ cm^{-2}. If we assume $A_V/N(^{13}\mathrm{CO}) = 4 \times 10^{-16}$ cm^2 mag (Dickman 1978), then the ^{13}CO gas column density implies $A_V = 64$ for Mon R2/IRS-3, in good agreement with the value derived from the silicate feature. We then convert our average value of $A_V = 72$ to N_H by assuming $N_H/\mathrm{A}_V = 1.9 \times 10^{21}$ cm^{-2} mag^{-1} (Mathis 1990). This implies $N_H = 1.4 \times 10^{23}$ cm^{-2} for Mon R2/IRS-3. Again there is some uncertainty in this because the value of N_H/A_V measured in the diffuse interstellar medium may not hold in molecular clouds. Our derived value of N_H implies that X(C–H) $= 1.3 \times 10^{-5}$ toward Mon R2/IRS-3. For a solar abundance of carbon, $X(\mathrm{C})/X(\mathrm{H}) = 3.6 \times 10^{-4}$ by number (Anders & Grevesse 1989), our estimate of X(C–H) implies that $\sim 4\%$ of the total carbon along the line of sight toward Mon R2/IRS-3 is locked in aromatic C–H bonds.

The total number of carbon atoms in aromatic hydrocarbons will be larger. If the absorbing aromatic hydrocarbons have the same size distribution as the emitting aromatic hydrocarbons, then we can use model results for the interstellar emission features to estimate the fraction, f, of the number of carbon atoms in aromatic C–H bonds, compared to the total number of aromatic carbon atoms. The value of f depends on the aromatic hydrocarbon size, with a smaller value for larger aromatic hydrocarbons. Désert, Boulanger, & Puget (1990) present a model of interstellar dust, including size distributions for different grain components and an analytic approximation for f as a function of radius a for PAH molecules. We have used their model, with a = 4–12 Å for PAHs, to calculate a size-averaged value for f of 0.40. The value of f for the absorbing aromatic hydrocarbons also depends on the degree of dehydrogenation in the interstellar medium, but aromatic hydrocarbons are predicted to be fully hydrogenated in molecular clouds shielded from ultraviolet radiation (Allamandola, Tielens, & Barker 1989). Thus the total amount of carbon in aromatic hydrocarbons is roughly a factor of ~2.5 times higher than the amount of carbon participating in aromatic C–H bonds. If the 3.25 μm feature is due to absorbing aromatic hydrocarbons with a size distribution similar to that adopted by Désert et al. (1990) for the emitting aromatic hydrocarbons in the interstellar medium, this would make the fraction of carbon in aromatic hydrocarbons ~9%. If the absorbing aromatic C–H bonds are instead attached to larger structures, for instance if the aromatic absorption is due to hydrogen on the surfaces of large amorphous carbon grains while the aromatic emission is due to small PAH molecules, then the fraction of carbon in such structures would be much larger than we estimate from the Désert et al. (1990) model.

Our estimate of the carbon abundance in aromatic hydrocarbons of $\sim$9% falls within the range of previous estimates for the aromatic hydrocarbon abundance, which vary from 0.8% to 18% of the total carbon abundance (Lepp et al. 1988; Allamandola et al. 1989; Puget & Léger 1989; Joblin, Léger, & Martin 1992). Thus if the 3.25 μm feature is due to aromatic hydrocarbons, we estimate that a significant fraction of carbon remains in aromatic hydrocarbons in molecular cloud dust.

If the 3.25 μm feature is due to, or contains contributions from, non-aromatic species, then the abundances of aromatic hydrocarbons along the line-of-sight derived above become upper limits. If it can be shown that *none* of the feature is due to aromatic hydrocarbons, then the abundance of carbon trapped in aromatic hydrocarbon molecules may be much lower in molecular clouds than in photodissociation regions or the diffuse interstellar medium. Aggregation of aromatic hydrocarbon molecules into larger graphitic-like structures is one possible explanation.

The most pressing need is to detect the 3.25 μm feature in other sources, both protostars and field stars behind molecular clouds. Brooke et al. (1995) have recently detected the 3.25 μm feature toward the protostars NGC 7538/IRS-1 and S 140/IRS-1, but observations are needed over a wider range of physical conditions. This will determine whether the feature arises in circumstellar environments or in the surrounding molecular cloud, and constrain the volatility of the absorber.

We would like to thank Dolores Walther for assistance with these observations, which were obtained during UKIRT Service Observing. We also appreciate useful conversations with Lou Allamandola, Christine Joblin, Scott Sandford, and Alan Tokunaga.

Table 1: Possible 3.25 Micron Feature Identifications

Source	Measured λ (μm)	Measured T (K)	Predicted λ at 80 K (μm)	Ref.
Mon R2/IRS-3	3.249 $\pm$ 0.004	80	3.249 $\pm$ 0.004	1
Mon R2/IRS-3	3.256 $\pm$ 0.003	80	3.256 $\pm$ 0.003	2
matrix-isolated coronene	3.257	4	3.257	3
gas-phase coronene	3.276	698	3.258	4
interstellar emission feature	3.289	1000	3.260	5
hydrogenated amorphous carbon	3.271	300	3.266	6
condensed coronene	3.290	788	3.268	4
matrix-isolated pyrene	3.268	4	3.269	3
quenched carbonaceous composite	3.289	300	3.285	7

References— (1) Sellgren et al. (1994); (2) this paper; (3) Joblin et al. (1994); (4) Flickinger et al. (1991); (5) Tokunaga et al. (1991); (6) Biener et al. (1994); (7) Sakata et al. (1990).

Note: The wavelength of these aromatic substances at a temperature of 80 K, appropriate for Mon R2/IRS-3 (Smith et al. 1989), was predicted from the measured wavelength and the temperature at which the wavelength was measured, using the temperature-dependent wavelength shifts measured by Joblin et al. (1995) for pyrene (for pyrene) or coronene (for all other substances). For the interstellar aromatic emission feature, we assumed a particle temperature of $\sim$1000K (Sellgren, Werner, & Dinerstein 1983).

REFERENCES

Allamandola, L. J., Tielens, A. G. G. M., & Barker, J. R. 1985, ApJ, 290, L25

Allamandola, L. J., Tielens, A. G. G. M., & Barker, J. R. 1989, ApJS, 71, 733

Allamandola, L. J., Sandford, S. A., Tielens, A. G. G. M., & Herbst, T. M. 1992, ApJ, 399, 134

Anders, E. & Grevesse, N. 1989, Geochim Cosmochim Acta, 53, 197

Beckwith, S., Evans, N. J., Becklin, E. E., & Neugebauer, G. 1976, ApJ, 208, 390

Biener, J., Schenk, A., Winter, B., Schubert, U. A., Lutterloh, C. & Küppers, J. 1994, Phys Rev B, 49, 17307

Blanco, A., Bussoletti, E., & Colangeli, L. 1988, ApJ, 334, 875

Brooke, T. Y., Sellgren, K. & Smith, R. G. 1995, ApJ, submitted

Colangeli, L., Mennella, V., & Bussoletti, E. 1992, ApJ, 385, 577

Désert, F. X., Boulanger, F., & Puget, J. L. 1990, A&A, 237, 215

d'Hendecourt, L. B., & Allamandola, L. J. 1986, A&AS, 64, 453

Dickman, R. L. 1978, ApJS, 37, 407

Flickinger, G. C., Wdowiak, T. J., & Gómez, P. L. 1991, ApJL, 380, L43

Grim, R. J. A., Greenberg, J. M., de Groot, M. S., Baas, F., Schutte, W. A., & Schmitt, B. 1989, A&AS, 78, 161

Hudgins, D. M., Sandford, S. A., Allamandola, L. J., & Tielens, A. G. G. M. 1993, ApJS, 86, 713

Joblin, C., Léger, A., & Martin, P. 1992, ApJL, 393, L79

Joblin, C., d'Hendecourt, L., Léger, A., & Défourneau, D. 1994, A&A, 281, 923

Joblin, C., Boissel, P., Léger, A., d'Hendecourt, L., & Défourneau, D. 1995, A&A, in press

Léger, A., & Puget, J. L. 1984, A&A, 137, L5

Lepp, S., Dalgarno, A., van Dishoeck, E. F., & Black, J. H. 1988, ApJ, 329, 418

Mathis, J. S. 1990, ARAA, 28, 37

Mitchell, G. 1995, private communication

Mountain, C. M., Robertson, D. J, Lee, T. J., & Wade, R. 1990, in *Instrumentation in Astronomy*, ed. D. L. Crawford, SPIE, 1235, 25

Nagata, T., Tokunaga, A. T., Sellgren, K., Smith, R. G., Onaka, T., Nakada, Y., & Sakata, A. 1988, ApJ, 326, 157

Ogmen, M. & Duley, W. W. 1988, ApJ, 334, L117

Puget, J. L. & Léger, A. 1989, ARA&A, 27, 161

Sakata, A., Wada, S., Onaka, T., and Tokunaga, A. T. 1990, ApJ, 353, 543

Sakata, A., Wada, S., Onaka, T., and Tokunaga, A. T. 1987, ApJ, 320, L63

Sellgren, K. 1994, in *The Infrared Cirrus and Diffuse Interstellar Clouds*, eds. R. M. Cutri and W. B. Latter (San Francisco: ASP), p. 243

Sellgren, K., Werner, M. W., & Dinerstein, H. L. 1983, ApJ, 271, L13

Sellgren, K., Smith, R. G., & Brooke, T. Y. 1994, ApJ, 433, 179

Smith, R. G., Sellgren, K., & Tokunaga, A. T. 1989, ApJ, 344, 413

Tokunaga, A. T., Sellgren, K., Smith, R. G., Nagata, T., Sakata, A., & Nakada, Y. 1991, ApJ, 380, 452

Williams, D. H., & Fleming, I. 1987, *Spectroscopic Methods in Organic Chemistry*, 4th ed. (McGraw-Hill: London), p. 41

Willner, S. P., et al. 1982, ApJ, 253, 174

This manuscript was prepared with the AAS LaTeX macros v3.0.

Figure Captions

Figure 1— New observations of the protostar Mon R2/IRS-3. Gaps in the data near 3.30 μm and 3.32 μm are due to Pfund δ in the standard star and strong telluric methane absorption, respectively. *Top*: the 3.16–3.55 μm spectrum (*histogram*) with a resolution of 0.0033 μm ($\lambda/\Delta\lambda = 1000$ at 3.25 μm). The units are flux density (F_λ) in W cm^{-2} μm^{-1} vs. wavelength in microns. A third-order polynomial (*solid curve*) was fit to the observations, excluding 3.2–3.3 μm and 3.4–3.6 μm from the fit, to determine the continuum. *Middle*: the 3.16–3.55 μm optical depth (*histogram*), compared to the sum of two Gaussians (*solid curve*), centered at 3.256 μm and 3.484 μm. The central wavelengths, widths, and optical depths of these two Gaussians were varied to produce the best fit to the data. *Bottom*: the 3.16–3.55 μm optical depth (*histogram*), compared to the profile of the aromatic interstellar emission feature (*solid curve*) in IRAS 21282+5050 (Nagata et al. 1988), after continuum subtraction (Tokunaga et al. 1991). The emission feature profile was first shifted to bluer wavelengths by 0.0294 μm to correct for temperature (see text and Table 1), and then scaled by the ratio of the average 3.17–3.28 μm optical depth of Mon R2/IRS-3 to the average 3.17–3.28 μm feature profile of IRAS 21282+5050.

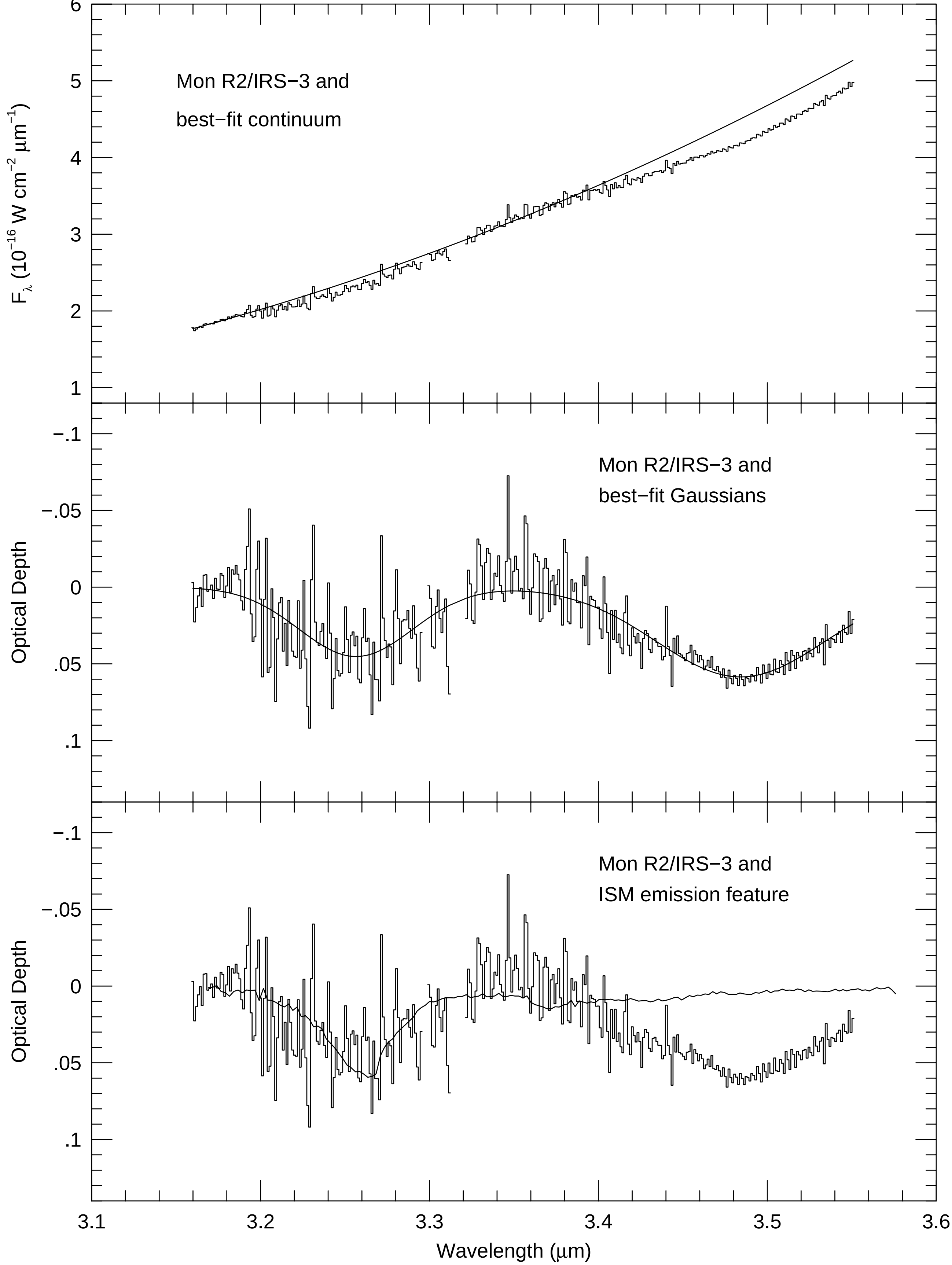

Mon R2/IRS−3 and
best−fit continuum
F_λ (10^{-16} W cm^{-2} μm^{-1})
Mon R2/IRS−3 and
best−fit Gaussians
Optical Depth
Mon R2/IRS−3 and
ISM emission feature
Optical Depth
Wavelength (μm)